Structure and vibrational spectra of carbon clusters in SiC

Alexander Mattausch,* Michel Bockstedte, and Oleg Pankratov

Lehrstuhl für theoretische Festkörperphysik, Universität Erlangen-Nürnberg, Staudtstrasse 7, 91058 Erlangen, Germany
(Received 26 July 2004; published 20 December 2004)

The electronic, structural, and vibrational properties of small carbon interstitial and antisite clusters are investigated by *ab initio* methods in 3*C*- and 4*H*-SiC. The defects possess sizable dissociation energies and may be formed via condensation of carbon interstitials, e.g., generated in the course of ion implantation. All considered defect complexes possess localized vibrational modes (LVM's) well above the SiC bulk phonon spectrum. In particular, the compact antisite clusters exhibit high-frequency LVM's up to 250 meV. The isotope shifts resulting from a ^{13}C enrichment are analyzed. In the light of these results, the photoluminescence centers D_{II} and $P-U$ are discussed. The dicarbon antisite is identified as a plausible key ingredient of the D_{II} center, whereas the carbon split interstitial is a likely origin of the $P-T$ centers. The comparison of the calculated and observed high-frequency modes suggests that the U center is also a carbon-antisite-based defect.

I. INTRODUCTION

Silicon carbide is a wide-band-gap semiconductor material especially suitable for high-power, high-frequency, and high-temperature applications. A common technique for the incorporation of dopant atoms into SiC is ion implantation. The post-implantation annealing is needed to reduce the damage. At the same time, the thermal treatment creates new stable defect centers that influence the material properties. The persistent centers that tend to grow even at annealing temperatures above 1000 °C are, e.g., the photoluminescence (PL) centers D_I (Ref. 1) and D_{II} (Ref. 2).

Most likely, the formation of these centers is related to the aggregation of the intrinsic defects. For example, vacancy or antisite clusters have been discussed[1,3,4] in conjunction with the D_I center. The D_{II} center, with its rich vibrational spectrum located above the SiC phonon spectrum, is considered as a carbon-related defect.[2,3,5] Until now, the complexity of the vibrational spectrum prevents an unambiguous identification of the microscopic structure. However, the theoretical investigations of the vibrational spectrum of small carbon clusters indicates that the dicarbon antisite (a carbon pair at the silicon site) is an important structural element of this defect.[5] Besides the D_{II} center, further carbon-related defects have been identified recently.[6,7] The photoluminescence centers $P-U$ appear in irradiated material and vanish between 1000–1300 °C.[6] Based on the analysis of ^{13}C isotope shifts of the localized vibrational mode (LVM) frequencies, a carbon split-interstitial model was suggested for the $P-T$ centers.[6] This proposal was recently questioned[8] and an alternative model was proposed. Generally, although the exact microscopic models for these defects remain to be established, it is clear that they are all due to the aggregation of carbon interstitials in smaller or larger clusters, which constitute a fundamentally important class of defects in SiC.

The finding that the carbon interstitials aggregate can help resolve a controversy regarding the formation of the persistent defect centers. Namely, the predicted high mobility of the carbon split interstitials[9,10] should hinder the formation of D_{II} centers at high temperatures[2,11] and opposes the thermal stability of the $P-T$ centers.[6] Due to high mobility, the carbon interstitials, which are a key ingredient of these centers,[2,5,6] should have vanished at elevated temperatures. Nevertheless, both features are observed experimentally. On the other hand, the recent tentative assignment[8,12–14] of the electron paramagnetic resonance (EPR) centers $T5$ in 3*C*-SiC (Ref. 15), and EI1 and EI3 (Ref. 16) in 4*H*-SiC to carbon split interstitials, which is based on the comparison of calculated and measured hyperfine parameters, supports the prediction of high mobility. These centers anneal between 150 and 240 °C. A low-temperature annealing of the silicon and carbon interstitials was also suggested for irradiated or implanted material by our theoretical analysis of competing annealing mechanisms.[13,17] The interstitial migration and the vacancy-interstitial recombination are activated at much lower temperatures than other mechanisms. We recently proposed[17] that small carbon aggregates may provide the missing link between the carbon interstitials and the persistent carbon-related defects. Such aggregates may trap interstitials at lower temperatures and reemit them again at higher temperatures, or even represent persistent photoluminescence centers themselves. Also in transient-enhanced dopant diffusion (TED) the carbon aggregates may serve as a source of carbon interstitials similarly to the so-called {311} defects in silicon,[18] which emit silicon interstitials and thereby facilitate the TED.

A thorough investigation of small and larger carbon aggregates should provide important information concerning their role in the annealing of implantation damage. The theoretical prediction of their vibrational spectra could also help to identify the microscopic structure of the PL centers. Yet, the assignment of a particular defect structure to PL centers from the phonon replicas alone is difficult. As additional information, the thermal stability and growth/annealing mechanisms of the clusters may be investigated by analyzing the dissociation energy of the defect complex and its preceding configurations. So far, theoretical investigations focused on di-interstitials and small interstitial clusters at antisites.[5,8] A detailed discussion of the vibrational signature of larger clusters is still missing.

In the present article we investigate the structure, dissociation energies, and vibrational properties of carbon interstitial and antisite aggregates and of larger clusters involving up to four carbon interstitials. We employ an *ab initio* method within the framework of density functional theory. The isotope shifts of defects with a distinct and clear splitting pattern are presented. Although theoretically all these defects can acquire different charge states, we focus on the neutral state as the most relevant for PL experiments. The PL due to bound excitons at a charged defect is unlikely to be seen as more nonradiative recombination channels are open in this case.[19] We have found high-frequency LVM's with up to 250 meV for small and compact defect clusters at antisites and LVM's up to 200 meV for interstitial clusters. As the cluster size increases, the frequency of the highest mode drops. In general, we find that the bond length between the involved carbon atoms, which is a measure of the bond strength, plays a crucial role. The analysis of further antisite-based clusters provides additional support for the previously suggested model of the dicarbon antisite as a core structure of the D_{II} center.[5] The vibrational signature and the isotope shifts of the split interstitial in the tilted configuration favor this defect as a candidate for the $P-T$ centers, although an assignment to the dicarbon antisite cannot be completely rejected. The existence of LVMs up to 250 meV for compact antisite clusters shows that the original suggestion of a completely carbon-based U center is possible. A comparison with theoretical results for diamond[20] reveals that interstitial defects with similar behavior as in SiC are also found in this structurally very similar material.

The article is organized as follows: Sec. II is denoted to a description of the method. In Secs. III and IV we present our results for interstitial and antisite clusters in detail and illustrate the rich variety of possible defect structures. In Sec. V the results will be discussed in the light of experimental and theoretical data. A summary concludes the article.

II. METHOD

Our first principles calculations have been carried out using the plane wave pseudopotential package FHI96SPIN[21] within the density functional theory (DFT) formalism.[22,23] The details of the method can be found in Ref. 9. For the expansion of the Kohn-Sham wave functions a basis set of 30 Ry cutoff energy is used. The exchange-correlation potential is taken in the local spin density approximation (LSDA).[24] For the calculation of the defect energetics large supercells with 216 lattice sites have been employed for $3C$-SiC and with 128 lattice sites for $4H$-SiC. The Brillouin zone has been sampled at the Γ point in $3C$-SiC, and in $4H$-SiC a $2 \times 2 \times 2$ Monkhorst-Pack mesh[25] has been used. All atoms in the cell have been allowed to relax.

The abundance of a defect under equilibrium conditions is given by its formation energy. However, as the radiative production of the defects is not an equilibrium process, the relevance of the formation energy is rather limited. For the formation and the stability of the carbon clusters in damaged material the dissociation energy is the more important quantity. It is defined as an energy needed to remove a single

atom from the defect. This quantity describes the thermal stability of a defect. In practice, for the carbon clusters, the dissociation energy is the energy difference between the total energy of the cluster and the total energy of the cluster with one carbon atom less plus the energy of an infinitely remote carbon interstitial:

$$E_{\mathrm{D}} = E_{\mathrm{tot}}(\mathrm{C}_{n-1}) + E_{\mathrm{tot}}(\mathrm{C}_{\mathrm{sp}}) - E_{\mathrm{tot}}(\mathrm{C}_n) \qquad (1)$$

Here C_{sp} denotes the $\langle 100 \rangle$ carbon split-interstitial, which is the energetically lowest carbon interstitial. Since the most stable configuration of the isolated carbon defect is used as the reference energy, Eq. (1) gives the lower bound of the dissociation barrier. We note that the tilted $\langle 100 \rangle$ split-interstitial configuration has been chosen, which is about 0.5 eV lower in energy than the symmetric $\langle 100 \rangle$ geometry.[9] The corresponding values of the formation energies are 6.7 eV in $3C$-SiC and 7.3 eV in $4H$-SiC. For all dissociation energies the neutral charge state has been assumed, as the carbon clusters are typically neutral in a typical range of the Fermi level (cf. Secs. III and IV).

The calculation of the vibrational modes has been performed in large supercells employing the defect molecule approximation. In this approximation the atoms belonging to the defect as well as the nearest neighbors are systematically displaced by about 0.15–0.7 % of the bond length and the dynamical matrix is calculated from the energy variation. The forces have been converged to a relative accuracy of 5 $\times 10^{-5}$. A detailed outline of the technique is given in Ref. 5. For the calculation of the dynamical matrix in $4H$-SiC the Brillouin zone has been sampled by the Γ point. It has been verified that the accuracy of the LVM calculation is not affected by this change. As we have shown earlier,[5] the main effect on the accuracy results from the uncertainty in the lattice constant (the lattice constant of the supercell including the defect differs slightly from that of the ideal lattice) and from the defect molecule approximation (which affects the energetically lowest LVM's close to the bulk spectrum). Due to the former the LVM's may change up to 10 meV when varying the lattice constant from the experimental value to the (smaller) theoretical LDA value. The latter results in a lowering of the energetically lowest LVM's. In some cases, referred to in the text, a 64-site cell has been used to calculate the LVM's. In these cases all atoms of the cell were included into the dynamical matrix.

The most important feature of PL centers is the zero phonon line (ZPL) that originates from a direct recombination of the bound exciton without involving the LVM's. Unfortunately, an analysis of the recombination process is beyond the capabilities of the static DFT-based methods. We therefore do not consider the recombination by itself, but focus on the vibrational modes as fingerprints of the particular carbon aggregates.

III. INTERSTITIAL CLUSTERS

Interstitial clusters are the simplest carbon aggregates. The original lattice structure is not altered, and no antisites or vacancies are needed for the cluster formation. The only prerequisite is an availability of carbon interstitials. Due to a

TABLE I. LVM's (in meV) and isotope shifts of the carbon split-interstitial dumbbell $C_{sp\langle 100\rangle}$ in the tilted configuration in 3C- and 4H-SiC. The values for 3C-SiC in parentheses are obtained using the defect-molecule approximation. As the tilted configuration of $C_{sp\langle 100\rangle}$ is asymmetric, the frequencies with only one substituted dumbbell atom depend on the orientation. The notation ^{12}C-^{13}C denotes the dumbbell configuration where the ^{13}C atom is sp^3 hybridized (cf. text).

Isotopes	3C				4H, cubic				4H, hexagonal					
	LVM	Ratio	LVM	Ratio	LVM	Ratio	LVM	Ratio	LVM	Ratio	LVM	Ratio	LVM	Ratio
^{12}C-^{12}C	188.7 (187.9)		120.4 (110.9)		186.6		111.3		192.9		124.1		122.5	
^{13}C-^{12}C	185.7 (185.0)	1.016	120.2 (109.7)	1.002 (1.011)	183.6	1.016	110.4	1.008	189.2	1.020	123.9	1.002	119.1	1.028
^{12}C-^{13}C	184.7 (183.9)	1.022	120.0 (109.2)	1.003 (1.016)	182.6	1.022	109.0	1.021	189.3	1.019	122.9	1.011	119.8	1.022
^{13}C-^{13}C	181.6 (180.8)	1.039	119.8 (108.0)	1.005 (1.027)	179.5	1.039	108.1	1.029	185.5	1.040	120.3	1.032	118.8	1.031

large formation energy of more than 6.5 eV the equilibrium concentration of these defects is well below the detectable limit. Hence the formation of the carbon clusters in a noteworthy concentration is possible only in irradiated or implanted material.

A. Carbon split interstitial

The carbon split interstitial C_{sp} (two carbon atoms sharing a single carbon lattice site) is the energetically lowest of the carbon interstitials. It possesses the charge states 2^+ to 2^-. As discussed in Ref. 9, the carbon split interstitial can be found in two different configurations. In positive charge states, the dumbbell is oriented in the $\langle 100\rangle$ direction and the defect has the D_{2d} symmetry, which may be lowered to D_2 due to the Jahn-Teller effect. In the symmetric configuration, two dangling p orbitals are oriented in $\langle 100\rangle$ direction. In the neutral and negative charge states, the defect gains about 0.5 eV by adopting a tilted structure compared to the metastable symmetric configuration. The $\langle 100\rangle$ dumbbell tilts by about 30°, so that one of the two carbon atoms acquires a sp^3 bonding configuration with the three silicon neighbors. In 4H-SiC two different configurations of the split interstitial should be considered. The alternating cubic and hexagonal planes in the 4H stacking sequence allows for two inequivalent sites—cubic and hexagonal—available to the defect. At a cubic site, the next-nearest-neighbor configuration is the same as in the zinc-blende structure, whereas at a hexagonal site it is of a wurtzite type. The tilt angles of the split-interstitial dumbbell in 3C-SiC and at the cubic site in 4H-SiC are similar. At the hexagonal site the tilt is also visible, but less pronounced. At both sites in 4H-SiC, the energy gain due to the tilt is only about 0.2 eV, which is less than in 3C-SiC. The driving force for the tilting is the stretching of the tetrahedron along the c axis already in the undistorted crystal, so that in 4H-SiC the undistorted configuration is closer to the tilted configuration than in 3C-SiC.

The tilted configuration of the split interstitial should be visible via the specific phonon replica in photoluminescence experiments. The calculated LVM's and the isotope shifts are listed in Table I. The calculation has been performed using full 64-site supercells with a special $2 \times 2 \times 2$ **k**-point sampling in 3C-SiC, whereas the defect-molecule approximation has been employed for 4H-SiC. For the 3C polytype we

found two vibrational modes above the SiC bulk phonon spectrum at 188.7 and 120.4 meV. A similar result is obtained for the split interstitial at the cubic site ($C_{sp,k}$). In this case we also find two LVM's at 186.6 and 111.3 meV. Since in 3C-SiC the defect-molecule approximation underestimates the frequency of the lower LVM by 10 meV (cf. Table I), we expect a similar shift of the modes in 4H-SiC. The higher LVM can be described as an isolated stretching vibration of the dumbbell, whereas the lower LVM is a concerted motion of the complete dumbbell against the elongated edge of the distorted tetrahedron. At the hexagonal site ($C_{sp,h}$), the vibrational pattern is slightly different. We obtain a stretching vibration with an energy of 192.9 meV, whereas there are two modes with energies 124.1 and 122.9 meV. They are also affected by the defect-molecule approximation; thus they are likely to rise in energy with the inclusion of additional surrounding shells in the calculation.[5] The nearly degenerate modes describe vibrations of one of the carbon atoms against its two silicon neighbors. The lifting of the degeneracy of these modes reflects the structural distortion, which is less pronounced at the hexagonal site than at the cubic site. These results may as well be transferred to 6H-SiC, which crystallizes with a hexagonal-cubic-cubic stacking. The cubic plane's environment is 3C-like, whereas for the hexagonal plane the same 2H-like structure as that for the hexagonal plane in 4H-SiC is present. Using the symmetric configuration of the split-interstitial, Gali et al.[8] obtained only a single LVM at 197 meV in 3C-SiC and at 183 meV for the hexagonal interstitial in 4H-SiC.

The calculated LVM's (including isotope shifts due to a substitution of one or both atoms with ^{13}C) are summarized in Table I. It is seen that the high-frequency LVM splits into four lines, with the two medium lines separated by only 1 meV. The frequency ratios for the shifted modes are close to the square root of the reduced mass ratios, which is 1.020 for the ^{12}C-^{13}C vibration and 1.041 for the ^{13}C-^{13}C vibration. For the low-frequency LVM, the two ^{12}C-^{13}C modes shift asymmetrically with the substitution of one carbon atom. The asymmetry is due to the tilted geometry of the defect. We observe in our results for 3C-SiC that the frequency ratio for this mode is affected by the defect-molecule approximation. When the full supercell is included into the calculation, the frequency shifts reduce to less than 1 meV,
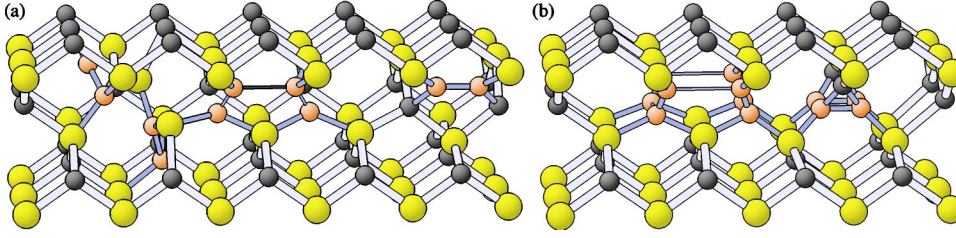
FIG. 1. Carbon-interstitial clusters in $3C$-SiC. (a) Carbon di-interstitials $(C_{sp})_{2,lin}$, $(C_{sp})_2$, and $(C_2)_{hex}$. (b) Carbon tetra-interstitials $(C_{sp})_4$ and $[(C_2)_{hex}]_2$.

resulting in a much lower frequency ratio. We expect a similar effect for the cubic site in $4H$-SiC.

B. Carbon di-interstitials

The unsaturated p orbitals of the interstitials enable the formation of stable di-interstitial complexes. As described in detail in Ref. 17, different forms of the di-interstitial are possible depending on the orientation of the neighboring interstitial sites. If the two interstitials are not contained within the {110} plane, a complex reconstruction occurs as depicted in Fig. 1(a), left. Since this defect consists of two tilted split-interstitials and a strongly displaced neighboring silicon atom, which results in a nearly linear geometry of carbon interstitials, we have labeled this di-interstitial $(C_{sp})_{2,lin}$ [for consistency with the di-interstitials in $4H$-SiC, we have

dropped the earlier notation $(C_{sp})_{2,tilted}$ of Ref. 17]. With 1.9 eV this defect possesses the lowest dissociation energy of all the di-interstitials in $3C$-SiC discussed here (cf. Table II). The di-interstitial $(C_{sp})_2$ [Fig. 1(a), center], which is comprised of two neighboring carbon split interstitials that are inclined towards each other, is more stable with a dissociation energy of 2.8 eV. The most stable reconstruction is $(C_2)_{hex}$ [Fig. 1(a), right] with a dissociation energy of 4.8 eV, where the di-interstitial is contained in a hexagonal ring. As the lattice geometry is only slightly distorted by this di-interstitial, the term $(C_2)_{hex}$ denotes that the di-interstitial is enclosed by a hexagonal ring. For this defect Gali *et al.* obtained a higher dissociation energy of 5.3 eV,[8] which, however, was calculated with a higher reference energy for the carbon interstitial.

TABLE II. Dissociation energy of the neutral carbon clusters. The given value is the energy needed to remove a single carbon atom. For the cluster type $(C_3)_{Si}$, the labels $I1$ and $I2$ refer to the metastable intermediate configurations, whereas the most stable triangular geometry is labeled $(C_{3,tri})_{Si}$. The two values for $(C_{sp})_{4,kkhh}$ in $4H$-SiC denoted with from hex. and from cub. are the energies needed to remove an atom from the hexagonal or cubic site, respectively.

| Cluster type		Dissociation energy (eV)			
$3C$-SiC					
$(C_I)_2$	$(C_{sp})_{2,lin}$	1.9		$(C_{sp})_2$	2.8
	$(C_2)_{hex}$	4.8			
$(C_I)_3$	$(C_2)_{hex}$-C_{sp}	0.4		$(C_{sp})_3$	3.0
$(C_I)_4$	$[(C_2)_{hex}]_2$	4.0		$(C_{sp})_4$	5.7
$(C_2)_{Si}$		4.1			
$(C_3)_{Si}$	$I1$	1.4		$I2$	3.6
	$(C_{3,tri})_{Si}$	4.8			
$(C_4)_{Si}$		2.8			
$[(C_2)_{Si}]_2$		5.9			
$4H$-SiC					
$(C_I)_2$	$(C_{sp})_{2,kk}$	2.5		$(C_{sp})_{2,hh}$	5.5
	$(C_{sp})_{2,kk,lin}$	4.6		$(C_{sp})_{2,hh,lin}$	4.6
	$(C_{sp})_{2,hk,cub}$	5.4		$(C_{sp})_{2,kh,hex}$	4.2
	$(C_2)_{hex,k}$	5.1		$(C_2)_{hex,k}$	5.1
$(C_I)_3$	$(C_{sp})_{3,kkh}$	2.9		$(C_{sp})_{3,khh}$	1.3
$(C_I)_4$	$(C_{sp})_{4,kkhh}$	5.3	(from hex.)		
		4.8	(from cub.)		
$(C_2)_{Si}$	$(C_2)_{Si,h}$	3.6		$(C_2)_{Si,k}$	3.5
$(C_3)_{Si}$	$I1$	1.9		$(C_{3,tri})_{Si,k}$	5.8
$(C_4)_{Si}$		2.9			
$[(C_2)_{Si}]_2$	$[(C_2)_{Si}]_{2,kh}$	6.7			
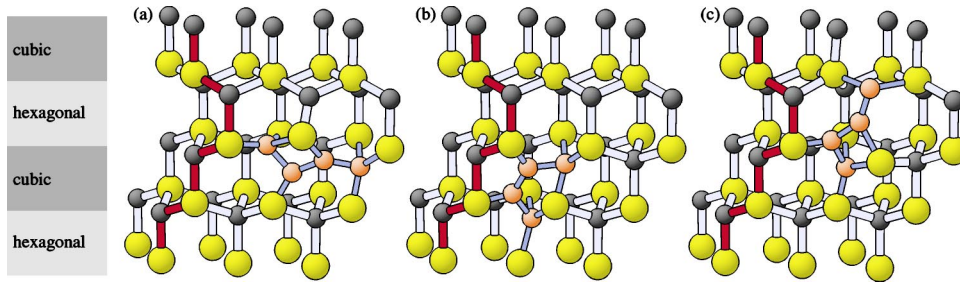
FIG. 2. Carbon di-interstitials in $4H$-SiC. (a) linear cubic-cubic di-interstitial $(C_{sp})_{2,kk,lin}$, (b) hexagonal-cubic di-interstitial in the cubic plane $(C_{sp})_{2,hk,cub}$, (c) cubic-hexagonal di-interstitial in the hexagonal plane $(C_{sp})_{2,kh,hex}$. The stacking order of the crystal is highlighted, the cubic and hexagonal planes are marked at the left.

The electronic structure of these defects has been discussed in Ref. 17. For a Fermi-level position around the midgap all di-interstitials are neutral. The di-interstitial $(C_{sp})_{2,lin}$ is neutral for $\mu_F > 0.8$ eV, $(C_{sp})_2$ for $\mu_F > 1.0$ eV, and $(C_2)_{hex}$ for all Fermi levels. The upper bound of the neutrality range could not be obtained, since the defect levels are resonant with the (artificially low) local density approximation (LDA) conduction band.

In $4H$-SiC a larger variety of di-interstitials is available. In addition to the various directions of the interstitial pair, the inequivalency of cubic and hexagonal sites has to be considered. In the stacking sequence of $4H$-SiC, the cubic $3C$-like and the hexagonal $2H$-like planes alternate (cf. Fig. 2). Hence a di-interstitial can comprise two cubic or two hexagonal sites in two different orientations. Figure 2(a) shows a di-interstitial on two cubic sites, which is comparable to $(C_{sp})_{2,lin}$ in $3C$-SiC, except that the two split interstitials show a much stronger relaxation towards each other. (Note that the c axis in $3C$-SiC is oriented along the $\langle 111 \rangle$ direction.) In this case the defect is totally contained within a cubic or hexagonal plane. Alternatively, the pair can reside on one cubic and one hexagonal site. Again, two different configurations are possible: the center of the di-interstitial may be contained in a $3C$-like cubic plane [Fig. 2(b)] or in a $2H$-like hexagonal plane [Fig. 2(c)]. Including di-interstitials within a hexagonal ring $[(C_2)_{hex}]$, which may reside in $4H$-SiC within a cubic or a hexagonal plane, eight different di-interstitial configurations can be counted in total, instead of only three in $3C$-SiC. They possess different dissociation energies (cf. Table II). The least stable structure is $(C_{sp})_{2,kk}$,

two split interstitials at neighboring cubic sites, whose geometry and dissociation energy of 2.5 eV are comparable to its $3C$-SiC counterpart. More stable are the cubic-hexagonal di-interstitial $(C_{sp})_{2,kh,hex}$ [cf. Fig. 2(c)] in the hexagonal bilayer with a dissociation energy of 4.2 eV, and the linear configurations $(C_{sp})_{2,kk,lin}$ and $(C_{sp})_{2,hh,lin}$ with dissociation energies of 4.6 eV. As in $3C$-SiC, the notation C_{sp} is used where the original carbon lattice atoms are strongly displaced and share their site with a carbon interstitial. The most stable configurations of the di-interstitial are those that are contained within a hexagonal ring. This is not only the case for both $(C_2)_{hex,k}$ and $(C_2)_{hex,h}$ (the hexagonal di-interstitials located in cubic and hexagonal planes), but also for $(C_{sp})_{2,kh,cub}$ [Fig. 2(b)] and $(C_{sp})_{2,hh}$. For the latter two configurations the di-interstitial is rotated so that it enters the neighboring hexagonal ring, which results in a structure similar to $(C_2)_{hex}$. The term C_{sp} in these di-interstitials reflects more the starting geometry than the final configuration, which is depicted in Fig. 2(b), since the two carbon interstitials relax strongly into the nearby hexagonal ring. With dissociation energies of 5.1 eV $[(C_2)_{hex}$ within the cubic and hexagonal plane], 5.4 eV $[(C_{sp})_{2,hk,cub}]$, and 5.5 eV $[(C_{sp})_{2,hh}]$, these di-interstitials are the most stable di-interstitial structures in $4H$-SiC. All defects are electrically neutral for the Fermi-level position between $\mu_F > 0.5$ eV and $\mu_F < 2.5$ eV.

The LVM's of the investigated interstitial clusters are listed in Table III. The di-interstitial's LVM's lie well above the SiC bulk phonon spectrum. With three high-frequency LVM's up to 185.1 meV $(C_{sp})_2$ possesses the simplest LVM

TABLE III. LVM's of neutral interstitial clusters in $3C$- and $4H$-SiC in meV. The values marked by an asterisk are slightly below the bulk phonon limit, which may be a result of the defect-molecule approximation. The edge of the bulk phonon spectrum obtained from *ab initio* calculations neglecting the macroscopic crystal polarization is 115.5 meV for $3C$-SiC and 118.6 meV for $4H$-SiC.

			$3C$					$4H$	
LVM	$(C_{sp})_2$	$(C_2)_{hex}$	$(C_{sp})_3$	$(C_{sp})_4$	$[(C_2)_{hex}]_2$	$(C_{sp})_{2,kk}$	$(C_{sp})_{2,hk,cub}$	$(C_{sp})_{2,hh}$	$(C_{sp})_{2,kk,lin}$
1	122.5	132.5	120.7	119.7	113.2*	123.7	128.0	134.9	117.1*
2	170.3	160.4	127.5	137.2	121.0	126.3	161.3	159.9	120.2
3	185.1	167.3	136.6	139.5	139.0	159.3	167.1	168.1	160.0
4		184.3	161.0	139.5	142.2	164.6	189.1	191.5	167.0
5			163.2	142.4	150.2				203.2
6					160.1				
7					194.7				
8					195.7				

spectrum. In $4H$-SiC this defect shows four LVM's with the highest mode at 164.6 meV, nearly 20 meV below its counterpart in $3C$-SiC. The reason for this frequency shift is the softening of the defect's bonds in $4H$-SiC. Indeed, the bond length between the split-interstitials is in $4H$-SiC about 0.11 Å longer than in $3C$-SiC. Gali *et al.*[8] obtained for the same defect in $3C$-SiC two high-frequency LVM's at 174 and 165 meV and four LVM's between 125 and 123 meV. The discrepancies in the high-frequency LVM's may be attributed to geometrical variations, whereas for the low-frequency LVM's this may be caused by the defect-molecule approximation. Yet, the spectrum structure is similar for all three defects: two relatively close high-frequency LVM's and LVM's close to the highest SiC bulk phonon mode. Also the vibrational pattern of the defects in $3C$-SiC and $4H$-SiC is similar. The two highest modes are the stretching vibrations of the two dumbbells (modes 2 and 3 in $3C$-SiC and modes 3 and 4 in $4H$-SiC in Table III). The low-energy modes involve vibrations against the nearest-neighbor atoms of the defect. In both polytypes the defect shows complex isotope shifts with an at least fivefold splitting of the highest LVM and an at least fourfold splitting of the second highest LVM, which partially overlap.

The di-interstitials $(C_2)_{hex}$ in $3C$-SiC and $(C_{sp})_{2,hk,cub}$ and $(C_{sp})_{2,hh}$ in $4H$-SiC reveal their common hexagonal nature also in their vibrational modes: the maximum deviation between the modes of the defects is about 7 meV, which lies within the accuracy of the method.[5] Due to their structural analogy, we expect similar results for the di-interstitials $(C_2)_{hex}$ within the cubic and hexagonal planes. The modes of the hexagonal di-interstitials reach up to 191.5 meV. This highest mode 4 is a stretching vibration of the two carbon atoms enclosed in the hexagonal ring, whereas the modes 2 and 3 are symmetric and antisymmetric stretching vibrations with the two adjacent carbon atoms. Mode 1 is a rotation of the two outer dumbbells against each other. The defects in $4H$-SiC show the same vibrational pattern. Comparable results have been found by Gali *et al.*[8] with LVM's at 190, 172, 166, 135, 133, and 117 meV. Again, the differences in the low-energy mode may be attributed to the defect-molecule approximation. Regarding the isotope shifts, the three defects $(C_2)_{hex}$ in $3C$-SiC and $(C_{sp})_{2,hk,cub}$ and $(C_{sp})_{2,hh}$ in $4H$-SiC also reveal their common nature. As expected for a stretching vibration of a carbon-carbon dumbbell, the highest mode shows a threefold isotope splitting. We obtain frequency ratios for all three defects of 1.016 for the medium ^{12}C-^{13}C line and 1.035 [$(C_{sp})_{2,hh}$, 1.034] for the ^{13}C-^{13}C line. The energetically lower modes show a complex broadening without a clear structure.

A different spectrum is obtained for the linear di-interstitial configurations, as displayed by $(C_{sp})_{2,kk,lin}$. The five LVM's reach up to 203.2 meV, which is attributed to the short bond length between the atoms of the linear carbon chain. The vibrational pattern of this defect is difficult to resolve. In general, the different modes of this defect are stretching vibrations of two neighboring carbon atoms against each other. The two outmost pairs are associated with the high-energy vibrations. The complex vibrational pattern leads to complex isotope shifts: the highest mode at

203.2 meV shows a sixfold and the second highest mode a fourfold splitting. The two lower modes broaden by up to 6 meV without structure.

C. Carbon tri- and tetra-interstitials

The di-interstitials can trap further carbon interstitials and form larger carbon aggregates. We investigated the growth of small carbon clusters of up to four carbon interstitials. We found that in $3C$-SiC the pair of carbon split interstitials $(C_{sp})_2$ binds additional carbon atoms most effectively. The reason is that the interstitial pair $(C_{sp})_2$ possesses dangling bonds located at the two sp^2-hybridized carbon atoms that point towards the adjacent carbon sites [cf. Fig. 1(a), center]. The dissociation energy of the resulting tri-interstitial $(C_{sp})_3$ amounts to 3.0 eV (cf. Table II). This defect exhibits a negative-U effect with an ionization level $\epsilon(2^+|0)=0.74$ eV and is negatively charged for $\mu_F > 1.5$ eV. The tri-interstitial may capture a further carbon interstitial and form a very stable tetra-interstitial $(C_{sp})_4$, whose dissociation energy amounts to 5.7 eV [cf. Fig. 1(b), left and Table II]. The high stability of $(C_{sp})_4$ originates from the complete sp^3 hybridization of all carbon interstitials, which also renders this defect electrically inactive.

The hexagonal di-interstitial $(C_2)_{hex}$ in $3C$-SiC is more stable than $(C_{sp})_2$. It can also trap additional carbon atoms, but with a smaller binding energy. An extra carbon atom at a neighboring carbon site, forming the tri-interstitial $(C_2)_{hex}$-C_{sp}, needs only 0.4 eV to separate. As a consequence, we expect the kinetic formation of tri-interstitials in the form of $(C_{sp})_3$, despite the higher stability of $(C_2)_{hex}$ compared to $(C_{sp})_2$. Since the reorientation from $(C_{sp})_2$ towards $(C_2)_{hex}$ involves the breaking of two carbon-silicon bonds, the capture of a third carbon interstitial may be possible before the reorientation occurs. The reorientation of $(C_{sp})_2$ into $(C_2)_{hex}$ and the capture of a third carbon interstitial are hence competing processes.

Once the tri-interstitial $(C_2)_{hex}$-C_{sp} has formed, adding a further carbon atom stabilizes the structure: the resulting tetra-interstitial $[(C_2)_{hex}]_2$ has a dissociation energy of 4.0 eV [cf. Fig. 1(b), right and Table II]. It consists of two neighboring hexagonal di-interstitials forming a rectangle with side lengths of 1.45 Å (di-interstitial within the hexagon) and 1.55 Å. The narrow sides of the rectangle form isosceles triangles with the neighboring carbon atom from the enclosing hexagon with a side length of 1.43 Å.

Similar interstitial clusters are also available in $4H$-SiC. Due to the enormous amount of possible configurations one has to restrict the analysis to some sample processes. Similar to $3C$-SiC, the aggregation at a hexagonal di-interstitial such as $(C_2)_{hex}$ results in the lowest formation energy. A split-interstitial bound to $(C_{sp})_{2,hh}$, which resembles—as mentioned above—a hexagonal di-interstitial, needs only 0.6 eV to dissociate. The di-interstitial $(C_{sp})_{2,kh}$ in a cubic plane traps carbon interstitials more effectively: the energy gain for a split-interstitial at a neighboring hexagonal site amounts to 1.3 eV (cf. Table II). As in $3C$-SiC the most efficient seed for the carbon aggregation is $(C_{sp})_{2,kk}$. The dissociation en-
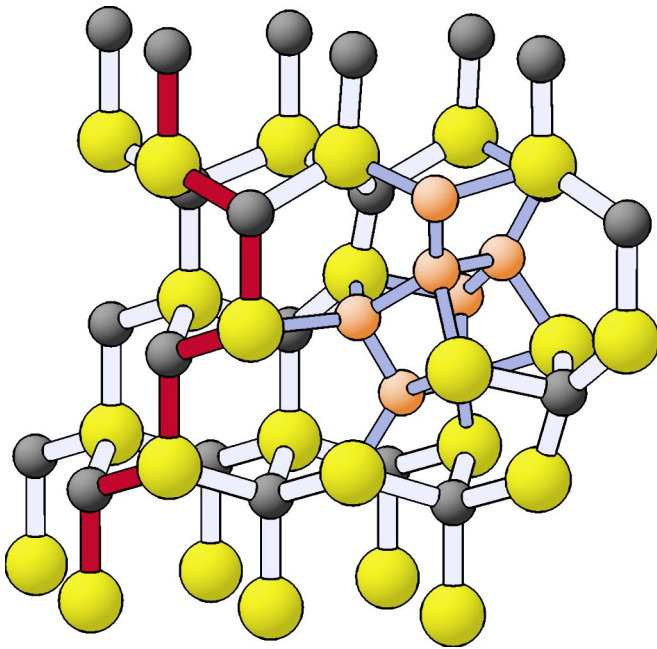
FIG. 3. Tetra-interstitial in $4H$-SiC spanning a cubic and a hexagonal plane. The stacking sequence of the crystal is highlighted.

ergy of $(C_{sp})_{3,kkh}$ located in the hexagonal plane amounts to 2.9 eV (cf. Table II)—a value comparable to the split-interstitial cluster $(C_{sp})_3$ in $3C$-SiC. With a fourth carbon interstitial another stable extended defect cluster is formed. The structure, spanning the cubic and the hexagonal plane, is shown in Fig. 3. The energy of 5.3 eV (4.8 eV) is needed to remove a carbon atom at a hexagonal (cubic) site. This defect has a different geometrical structure than $(C_{sp})_4$ in $3C$-SiC. However, all atoms are also sp^3 hybridized, which again leads to the high stability of the complex. Further defect structures can exist in $4H$-SiC due to the alternating cubic and hexagonal planes. We expect similar dissociation energies for all these defects.

We analyzed the LVM's of the tri-interstitial $(C_{sp})_3$ and the tetra-interstitials $(C_{sp})_4$ and $[(C_2)_{hex}]_2$ in $3C$-SiC. All defects show vibrational modes above the SiC bulk phonon spectrum, but for $(C_{sp})_3$ and $(C_{sp})_4$ the frequency of the highest mode decreases with the number of atoms. The reason is that the bond length between split interstitials increases and the bonding is weakening. Starting with the di-interstitial, the highest LVM drops from 185 to 163 meV for $(C_{sp})_3$ and 142 meV for $(C_{sp})_4$ (cf. Table III). The highest modes 3 and 4 for $(C_{sp})_3$ are antisymmetric and symmetric stretching vibrations of the two split interstitials located at the border of

the triangle-shaped defect complex. Modes 2 and 3 are also antisymmetric and symmetric vibrations of the pairs that form the sides of the triangle, whereas in mode 1 the center split interstitial vibrates against its outer neighbors. The highly symmetric structure of $(C_{sp})_4$ is also reflected in the LVM's: the highest mode 5 describes a stretching vibration of all split interstitials where two neighboring interstitials are always in opposite phase. Modes 3 and 4 are degenerate and represent an antisymmetric vibration of two opposite split interstitials, respectively. In mode 2 the long carbon-carbon bonds between two neighboring split interstitials are stretched and in mode 1 the diagonally opposite split interstitials rotate against each other.

The complex $[(C_2)_{hex}]_2$ shows a rich spectrum of eight LVM's up to 196 meV. The reason for these high-frequency LVM's is the compact size of the defect. The two highest modes 7 and 8 are symmetric and antisymmetric stretching vibrations of the two triangles. Modes 5 and 6 are a symmetric and antisymmetric tilting of the narrow sides of the rectangle against the third carbon atoms in the triangles. Mode 4 describes a breathing vibration of the rectangle combined with an oscillation of the carbon atoms at the triangles' apex against each other, whereas mode 3 is an antisymmetric stretching and quenching of the two triangles. The low-frequency modes 1 and 2 are complex oscillations, which presumably extend beyond the analyzed defect molecule.

IV. ANTISITE CLUSTERS

The carbon antisite has a formation energy of 4.2 eV (Si-rich conditions) in $3C$-SiC as well as in $4H$-SiC. Alongside with the carbon vacancy, it is the energetically most favorable intrinsic defect. Various antisite formation mechanisms have been suggested so far: the recombination of the V_C-C_{Si} complex with a silicon atom,[26] a kick-out mechanism,[4] the recombination of a carbon interstitial with a silicon vacancy, and the incorporation in as-grown material are likely. Unfortunately, this defect is hardly detectable: neither does it possess defect states in the band gap, nor does it show localized vibrational modes.[26] Nevertheless, the carbon antisite is of particular importance as a nucleus for larger carbon aggregates. It may capture carbon interstitials and form small, tightly bound complexes that may be featured as various thermally stable defect centers.[5,8,26,27]

A. Dicarbon antisite

The simplest and most discussed defect of this kind is the dicarbon antisite $(C_2)_{Si}$,[5,8,26–28] where two carbon atoms
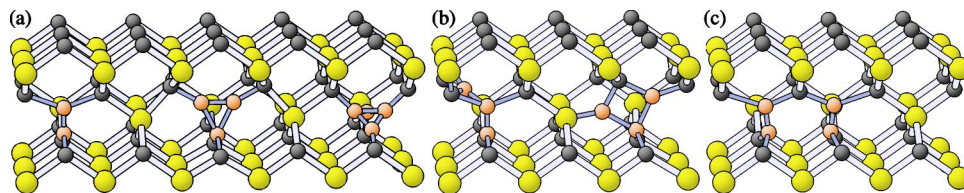

FIG. 4. Aggregation of carbon clusters at a carbon antisite in $3C$-SiC. (a) Dicarbon antisite $(C_2)_{Si}$, tricarbon antisite $(C_3)_{Si}$, and tetracarbon antisite $(C_4)_{Si}$. (b) Intermediate configurations $I1$ and $I2$ of the tricarbon antisite. (c) Pairing of two dicarbon antisites $[(C_2)_{Si}]_2$.

TABLE IV. LVM's of carbon-antisite clusters in $3C$ and $4H$ in meV. The subscripts k and h denote the cubic and the hexagonal site. The second values for $(C_2)_{Si}$ $(3C)$ are from the calculation of a full 216-site cell in a symmetric high-spin configuration. The results for $(C_2)_{Si,h}$ in $4H$-SiC are similar to $(C_2)_{Si,k}$ and given in Ref. 5. The values marked by an asterisk are slightly below the bulk phonon limit, which may originate from the employed defect-molecule approximation. The bulk phonon limit obtained from *ab initio* calculations without macroscopic crystal polarization is 115.5 meV for $3C$-SiC and 118.6 meV for $4H$-SiC.

	$3C$						$4H$				
LVM	$(C_2)_{Si}$	$(C_3)_{Si}$	$(C_4)_{Si}$	$[(C_2)_{Si}]_2$	$[(C_2)_{Si}]_{2,hex}$	$[(C_2)_{Si}]_4$	$(C_2)_{Si,k}$	$(C_3)_{Si,k}$	$(C_4)_{Si,k}$	$[(C_2)_{Si}]_{2,kh}$	$[(C_2)_{Si}]_{2,hh}$
1	116.4	118.6	124.7	123.3	118.6	116.3	102.3*	119.0	113.4*	114.4*	114.3*
2	128.5/125.5	129.8	130.6	125.6	134.0	116.4	119.7	130.2	114.3*	119.6	120.4
3	139.4/143.2	148.7	138.0	127.1	138.3	117.6	135.0	154.0	114.5*	132.2	130.8
4	148.3/144.2	181.3	165.8	139.3	164.1	119.7	139.1	182.3	120.3	147.0	145.7
5	177.5/178.3	248.5	181.2	168.6	170.1	121.5	178.0	254.9	200.1	160.2	159.7
6			189.4	169.7	174.2	121.6			201.5	162.4	161.8
7			223.6			124.1			204.3		
8						138.5			240.7		
9						141.0					
10						142.2					
11						142.9					

share a single silicon site (cf. Fig. 4, left). It exists in $3C$- and $4H$-SiC and has a dissociation energy of 4.1 eV in $3C$-SiC and 3.5 eV (3.6 eV) in $4H$-SiC at the cubic (hexagonal) site (cf. Table II). The defect is neutral in the Fermi-level range of $0.76 < \mu_F < 1.11$ in $3C$-SiC and $1.27 < \mu_F < 2.04$ in $4H$-SiC. It can prevail in a high-spin state and a Jahn-Teller distorted low-spin state. The high-spin state is favored by 80–120 meV, whereas this energy difference is too low to uniquely determine the ground state. We have discussed the structural, electronic, and vibronic properties of this defect in detail in Refs. 5, 26, and 28. Here we present the results for the LVM's isotope shifts of this defect. The LVM's of $(C_2)_{Si}$ for $3C$-SiC and $4H$-SiC are listed in Table IV. For the former the results of the Jahn-Teller distorted configuration in a 64-site cell and the results for a high-spin nearly symmetric configuration in a

216-site cell are given. The results for $4H$-SiC are for the low-spin state and have been calculated in a 128-site cell using the defect-molecule approximation (the results for the high-spin state are given in Ref. 5). In Fig. 5 we show the isotope effect for LVM's of $(C_2)_{Si}$ in $3C$-SiC assuming a ^{13}C enrichment of 30%. We included the dumbbell and its four nearest neighbors in the calculation and assumed that ^{13}C can substitute with equal probability of 30% any of these sites. Note that the height of the peaks in Fig. 5 does not necessarily reflect the line intensity in the photoluminescence experiments. We find that similar to the carbon split interstitial the energetically highest mode 5 splits into three lines. The reason is the strong localization of the vibration on the carbon dumbbell. The middle shifted line, with a ratio of 1.019 to the highest line in the isotope-undoped sample, results from the vibrations of the
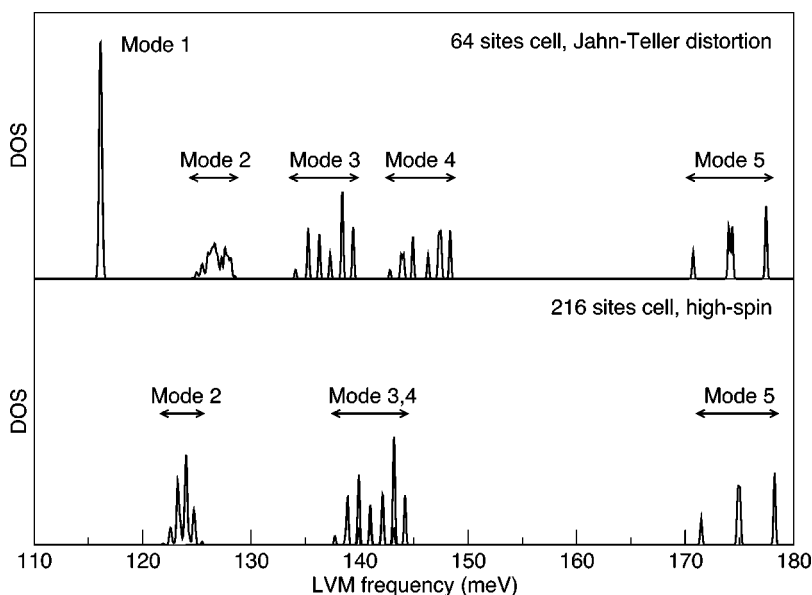

FIG. 5. Isotope shifts of the dicarbon antisite enriched with 30% [13]C. The upper panel shows the splitting of the modes calculated in a 64-site supercell in the Jahn-Teller distorted configuration, the lower in a 216-site supercell with a high-spin-like symmetric configuration. The frequencies of the pure ^{12}C case are given in Table IV.

^{12}C-^{13}C dumbbell, whereas the lowest line, shifted by 1.040, comes from the ^{13}C-^{13}C dumbbell. This result is identical for both high-spin and Jahn-Teller distorted configurations. Modes 3 and 4, which are vibrations of the upper and lower parts of the dumbbell against the neighbors, split into six nearly equidistant lines with separations between 1 and 1.4 meV. In the Jahn-Teller distorted case (cf. upper panel of Fig. 5), the two shifted spectra are clearly separated; in the symmetric high-spin case (cf. lower panel of Fig. 5) they overlap and show a distinct signature of six lines. The mode 2 shows a broadening with two maxima at 127.6 and 126.7 meV in the distorted case four peaks in the symmetric configuration. In the former, the whole width of the broadening reaches from 128.5 to 124.9 meV. The ratios of the two maxima compared to the ^{12}C value are 1.007 and 1.014. The four modes of the latter reach from 124.8 to 122.6 meV. Mode 1, which is the breathing mode in Jahn-Teller configuration, remains practically undisturbed by the ^{13}C enrichment. This mode, however, drops into the bulk continuum for the high-spin case.[5]

B. Clusters of dicarbon antisites

Another defect, which is closely related to the dicarbon antisite, is the dicarbon-antisite pair $[(C_2)_{Si}]_2$ [cf. Fig. 4(c)]. Like the dicarbon antisite, this defect has already been discussed in earlier publications.[5,8] Here we want to compare our results for the dicarbon-antisite pair with the structurally very similar di-interstitials. For the formation of dicarbon-antisite pairs, the lone pairs or other clusters of antisites have to be created first. Eberlein *et al.*[4] suggested the antisite formation via kick-out reactions. Rauls *et al.*[29] discussed a vacancy-mediated mechanism. The structural difference of the dicarbon-antisite pair from the carbon di-interstitial is in the carbon-dominated environment. The same defect configurations are available for the dicarbon-antisite pair as for the di-interstitial. The defect spans two neighboring sites of the same sublattice, hence in $4H$-SiC the same variety of different configurations can form: cubic-cubic, hexagonal-hexagonal in two different orientations and cubic-hexagonal within the cubic and the hexagonal plane. Also a variant comparable to $(C_2)_{hex}$ is available which we label $[(C_2)_{Si}]_{2,hex}$. It can be visualized as a hexagonal di-interstitial [Fig. 1(a), right] with a carbon environment. The dicarbon-antisite pair is very stable: the energy of 5.9 eV is needed to remove a carbon atom in the $3C$-SiC polytype. This dissociation energy is identical for $[(C_2)_{Si}]_2$ and the hexagonal dicarbon antisite $[(C_2)_{Si}]_{2,hex}$, thus neither configuration is energetically preferred. In $4H$-SiC, the dissociation energy of as much as 6.7 eV is obtained for the cubic-hexagonal configuration in the cubic plane (Fig. 6). Alongside the hexagonal-hexagonal configuration, this is the most stable defect. The calculation of the dissociation energy for all types of the defect would be too costly. Thus we evaluated the formation energies of the defects. The formation energy of the cubic-cubic complex is about 0.3 eV higher than the hexagonal-hexagonal configuration, followed by the linear structures as described for the di-interstitial (hh, 0.7 eV; kk,
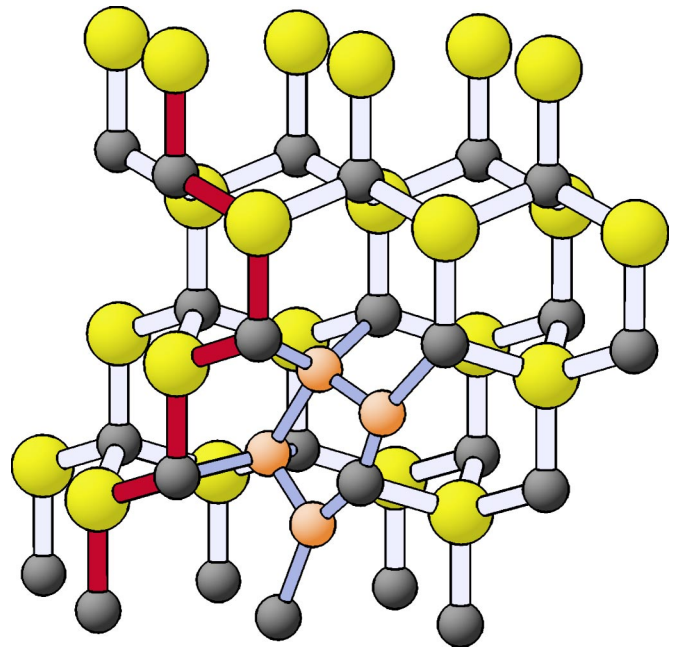

FIG. 6. Pair of dicarbon antisites $[(C_2)_{Si}]_{2,kh}$ in $4H$-SiC spanning cubic and hexagonal sites in the cubic plane. The stacking sequence of the crystal is highlighted.

1 eV) and the cubic-hexagonal defect in the hexagonal plane (1.2 eV). The higher binding energy in $4H$-SiC compared to $3C$-SiC originates from the enhanced relaxation. The defects thus benefit from the larger room for the relaxation due to the alternating cubic and hexagonal planes. Apart from the formation energy, the defect concentration also depends on the availability of adjacent carbon antisites and can be kinetically limited.

The LVM's of $[(C_2)_{Si}]_2$ in $3C$- and $4H$-SiC are given in Table IV. A detailed description of the modes is presented in Ref. 5. Remarkable is the polytype-independent small splitting of modes 5 and 6, which is observed for all configurations of the dicarbon-antisite pair. Similar results are obtained for the cubic-cubic configuration, which is not listed in Table IV. For this defect, the LVM's differ by at most 2 meV from the values of the hexagonal-hexagonal configuration. The isotope splitting of all configurations is complex. The defect does not possess isolated dumbbell oscillations, and the LVM's 5 and 6 are very close. Consequently, the isotope shifts of the two highest LVM's overlap, resulting in broad peaks with a width of up to 2.5 meV, which cannot be clearly separated.

The hexagonal dicarbon-antisite pair $[(C_2)_{Si}]_{2,hex}$ shows vibrational properties similar to the hexagonal di-interstitial. The highest LVM at 174.2 meV is practically an isolated dumbbell vibration, whereas the small splitting between the modes 5 and 6 is typical for $[(C_2)_{Si}]_2$. Mode 5 is a rotation of the dumbbell in the plane of the nearest neighbors. The lower modes are complex vibrations of the entire carbon surrounding. The complex vibrational pattern is reflected in the isotope splittings. Mode 6 shows a threefold carbon dumbbell splitting, where the medium mode is again split into two separate lines with a 0.5-meV energy difference. The fre-

quency ratios are 1.013 (averaged over the two lines—1.011 and 1.015 otherwise) and 1.031. This is, however, superimposed with the complex splitting pattern of modes 4 and 5. Thus an extensive isotope broadening between 160 and 175 meV is expected for this defect.

Larger aggregations of dicarbon antisites are also conceivable. Similar to the tetracarbon interstitial cluster, the complex of dicarbon antisites can be imagined. Provided the lone antisites are formed kinetically, the antisite cluster is strongly bound: the energy of 7.4 eV is needed to remove a carbon atom from $[(C_2)_{Si}]_4$. The defect is electrically inactive, similar to its interstitial counterpart. It possesses 11 LVM's above the SiC bulk phonon spectrum. Similarly to the tetra-interstitial $(C_{sp})_4$ four modes lie between 138.5 and 142.9 meV (cf. Tables III and IV). The additional modes in the low-frequency range up to 124.5 meV originate from the stronger carbon-carbon bonds. The bonds are, however, elongated compared to the dicarbon-antisite pair due to the practically undistorted original SiC surrounding.

C. Tri- and tetracarbon antisites

In addition to the clustering, the dicarbon antisites can trap carbon interstitials. Examples are the tricarbon and the tetracarbon antisite [cf. Fig. 4(a), center and right]. Both are tightly bound defects with three or four carbon atoms at a single silicon site.

The tricarbon antisite is a triangle-shaped defect with its base oriented in the $\langle 110 \rangle$ direction. The capture of a carbon interstitial by the dicarbon antisite yields the energy of 4.8 eV (cf. Table II). This capture may occur via several intermediate configurations, which are depicted in Fig. 4(b). First, a carbon interstitial is trapped at a neighboring carbon site [Fig. 4(b), left, configuration $I1$] with an energy of 1.4 eV. This is about 1 eV higher than the migration barrier for the neutral carbon split interstitial.[9] In a second step, a square configuration of the tricarbon antisite may form [cf. Fig. 4(b), right, configuration $I2$], with the additional energy gain of 2.2 eV ($E_D = 3.6$ eV). This configuration is metastable and has also been found by Gali *et al.*[8] with a dissociation energy of 4.0 eV. In a last step, the triangular configuration is finally formed [configuration $(C_{3,tri})_{Si}$], yielding an additional 1.2 eV. This process is also possible in 4H-SiC—an adjacent split interstitial to the dicarbon antisite is bound with 1.9 eV (configuration $I1$ in Table II), yielding an additional energy gain of 3.8 eV in the triangular configuration [$E_D = 5.8$ eV, configuration $(C_{3,tri})_{Si}$]. In its first formation step the tricarbon antisite is electrically neutral for $\mu_F > 0.7$ eV. This value reduces in the next steps.

The defect shows a pronounced LVM spectrum (cf. Table IV): the five modes reach up to 248.5 meV (255.1 meV in 4H-SiC). This is the highest value among all defects we have analyzed. This is also much higher than the LVM's in the intermediate configuration [Fig. 4(b), right] obtained by Gali *et al.*[8] at 190, 172, 166, 135, 133, and 117 meV. The reason for the high frequency is the short bond length between the adjacent carbon atoms—it ranges from 1.29 Å for the base of the triangle to 1.55 Å for the distance between

the triangle's apex and the carbon atoms of the enclosing tetrahedron. The highest mode (mode 5) is a stretching vibration of the short base of the triangle. Mode 4, which is with 181.3 meV still very high, is an asymmetric stretching vibration of the two base atoms against their nearest neighbors from the enclosing tetrahedron. In mode 3 the triangle is stretched, whereas in mode 2 the whole triangle oscillates against the tetrahedron. Mode 1 is a vibration of the carbon atom at the apex against its neighbors.

Since mode 5 is strongly localized at the base of the triangle, one expects a very distinct pattern of isotope shifts similar to the isolated carbon dumbbell. Indeed, replacing the nearest neighbors of the triangle with ^{13}C does not affect this mode at all. Thus the analysis of the isotope shifts for this mode can be restricted to the defect itself. Three frequencies are obtained: 248.5 meV for the pure ^{12}C case (248.3 meV if the carbon atom at the apex is substituted), 244.3 meV if one of the two carbon atoms of the base is replaced by ^{13}C and 239.8 meV in the ^{13}C-^{13}C case. The corresponding ratios are thus 1.018 and 1.036, respectively. In 4H-SiC, we find the shifted lines at 250.5 and 246.0 meV, with frequency ratios of 1.017 and 1.036. As discussed above, the energetically lower modes have complex vibrational patterns involving also the nearest-neighbor atoms of the defect. As seen for the dicarbon antisite, only a broadening of the modes and not such a distinct splitting will result from substituting the defect's atoms with ^{13}C.

With the capture of another carbon interstitial the tetracarbon antisite $(C_4)_{Si}$ is formed [cf. Fig. 4(a), right]. With the dissociation energy of 2.8 eV in 3C-SiC and 2.9 eV in 4H-SiC (cf. Table II) this defect is less stable than $(C_3)_{Si}$, but still tightly bound. In 3C-SiC, the central carbon dumbbell is oriented in {110} direction having two additional carbon atoms at each side. The dumbbell is 1.70 Å long, the sides of the two isosceles triangles formed by the dumbbell and the additional carbon atoms are 1.38 and 1.44 Å, respectively. For a Fermi level $\mu_F > 0.6$ eV and $\mu_F < 1.5$ eV the defect is neutral. The asymmetric geometry is the result of a Jahn-Teller effect. In the symmetric configuration, the defect possesses a doubly degenerate localized state in the band gap. Since in the neutral state this level is occupied, the symmetry is broken by a Jahn-Teller distortion, which yields an energy gain of about 1 eV. The asymmetric configuration gives rise to a rich LVM spectrum with high-frequency LVM's. We have found 7 LVM's above the bulk spectrum with the highest LVM at 223.6 meV. Mode 7 is a stretching vibration of the smaller of the two triangles. The atom at the apex oscillates against the central dumbbell and the carbon atom of the enclosing tetrahedron. Mode 6 is an antisymmetric stretching vibration of the two atoms of the central dumbbell atoms against their neighbors. Since the vibration is antisymmetric, the length of the central dumbbell remains constant. Mode 5 is a stretching vibration of the second triangle with the larger sides, whereas mode 4 is mainly a stretching vibration of the lateral carbon farther away from the central dumbbell against its neighbor along the z axis. Modes 1 to 3 describe a complex motion of the inner carbon atoms against the enclosing tetrahedron. We find an at least sixfold isotope splitting of the highest

mode and a structureless broadening of the lower modes.

The tetracarbon antisite in $4H$-SiC shows a simpler LVM spectrum with only five LVM's above the bulk phonon spectrum. This is due to the highly symmetric defect geometry, which is, as mentioned above, not stable in $3C$-SiC. In the low-symmetry $4H$ crystal, the degeneracy of the defect states is lifted already in the symmetric configuration. The defect forms a small tetrahedron with a side length of 1.43 Å, which is enclosed in the carbonic tetrahedron of the crystal lattice. The highest mode 8 is found at 241 meV, followed by three nearly degenerate modes between 200 and 205 meV. Mode 8 is the breathing mode of the tetrahedron. Modes 5–7 are nearly degenerate and cannot be separated into vibrations of individual carbon pairs. The low-frequency modes 1 to 4 show complex vibrational patterns involving all atoms of the defect and the environment. These modes are the least localized. With the partial substitution by ^{13}C, the mode 8 splits into at least four lines separated by about 2 meV. The modes around 200 meV broaden into a continuum about 10 meV wide.

V. DISCUSSION

The calculated vibrational spectra advise a comparison with photoluminescence experiments. Several defect centers, which have been attributed to intrinsic defects, may be relevant. There are the alphabet lines,[30] the D_I center,[1] the D_{II} center,[2] and the recently discovered PL centers P–U.[6] However, the alphabet lines and the D_I center possess LVM's only in the phonon band gap. Hence the defects considered above are not suitable candidates. We will thus focus on the centers with vibrational modes above the SiC bulk phonon spectrum.

A. The D_{II} center

The D_{II} center shows vibrational modes above the SiC bulk spectrum up to 164 meV, which are to a large extent polytype independent.[31] Five modes have been described as "universal" throughout the polytypes. Yet, a comparison of the spectra for different polytypes indicates that, in fact, a larger number of modes can be regarded as polytype independent.[5] The number of reported LVM's varies. Five to six modes with tiny peaks in-between have been counted in $3C$-SiC and up to 12 modes have been observed in $4H$-SiC.[32] Another important feature is the thermal stability of the center: it persists temperatures up to 1700 °C.[2,11,31] First we summarize our results of Ref. 5 related to the dicarbon antisite (Sec. IV A) and to the dicarbon-antisite pair (Sec. IV B). In this context, we consider the new information concerning the larger defect clusters.

The dicarbon antisite possesses an LVM pattern compatible with the universal spectrum of the D_{II} center.[26] The high dissociation energy suggests a high thermal stability of this defect. Yet, the large number of LVM's in the hexagonal polytypes cannot be reproduced. Therefore, a larger complex, i.e., the dicarbon-antisite pair, has been proposed by Gali *et al.*[8] The idea was that the combination of the cubic and the hexagonal sites could explain the rich multitude of ZPL's in $4H$- and $6H$-SiC. However, also this model does

not explain in full the features of the D_{II} center.[5] Especially, it predicts a small splitting of the two highest LVM's (cf. Table IV) for all polytypes and all combinations of the site pairs, which is not observed in the D_{II} spectrum. In addition, the number of LVM's is still too low to explain the D_{II} spectrum in hexagonal polytypes. In an experimental paper,[33] it was suggested that the multiple ZPL's stem from the excited defect states. Yet, the dicarbon-antisite model qualitatively reproduces the most robust features of D_{II}. In general, the carbon-antisite-related defects possess LVM's in necessary frequency range. One can thus expect the dicarbon antisite to be a major building block or precursor of the D_{II} center. However, the dicarbon antisite itself and the dicarbon-antisite pair are too small to explain the whole vibrational spectrum. A larger defect structure seems indispensable, which could also account for the polytype-independent features.

On the other hand, the interstitial clusters as the model for the D_{II} center can be ruled out. None of the clusters shows a proper LVM spectrum. For the di-interstitials, a few LVM's above 160 meV exist, as well as a mode around 130 meV. The highest LVM has the tendency to drop with growing cluster size. Therefore, adding further interstitials would not improve the situation. On the contrary, the carbon-rich environment due to the incorporation of antisites provides the diamondlike spectrum of the D_{II} center. This is seen for the clusters at a single antisite and the dicarbon-antisite aggregates: the trapping of further carbon interstitials yields very short carbon-carbon bonds with high-frequency LVM's above 200 meV, whereas a clustering of dicarbon antisites results in a dropping of the highest mode, but also an increase of the number of LVM's. The combination of both processes may thus explain the LVM spectrum of the D_{II} center.

B. The P–T centers

Further intrinsic defects with high-frequency LVM's are the five centers labeled P–T, which were found in electron-irradiated $6H$-SiC.[6] An electron beam with the energy below the silicon displacement threshold, but at a very high dose of $3 \times 10^{20}e$ cm^{-2} was used. The five centers possess separate ZPL's with LVM's at 133 and 180 meV. The P center is the most stable and persists annealing temperatures of 1000 °C. Isotope-enriched PL measurements with a ^{13}C incorporation of 30% were performed. The higher LVM splits into three lines, with the isotope-undoped line shifted to about 175 and 171 meV. This results in frequency ratios (averaged over the five different centers) of 1.020±0.002 and 1.043±0.002. This isotope splitting has been interpreted as a vibration of a carbon-carbon dumbbell. For this defect the stretching vibration shows a threefold isotope splitting. The experimental results are in agreement with the square root dependence on the reduced mass. The ratios of the vibrational frequencies of a ^{12}C-^{13}C and a ^{13}C-^{13}C dumbbell to the frequency of the pure ^{12}C case are 1.020 and 1.041, respectively. A simple shift to 128 meV has been observed for the lower LVM. This yields a frequency ratio of 1.034±0.001. For the interpretation of this mode the oscillation of the carbon atom against

its silicon neighbors in a Si-C-Si molecule has been considered, which gives a frequency ratio of 1.033. This underlies a carbon split-interstitial model proposed for the *P–T* centers.

According to our calculations, the split interstitials (Sec. III A) and the dicarbon antisite (Sec. IV A) possess vibrational modes close to the LVM's of the *P–T* centers. The originally suggested split interstitial[6] has a single LVM above the SiC bulk spectrum in the symmetric case [219.2 meV in the charge state 2^+ (Ref. 26) and 183 meV in the neutral charge state[8] in $3C$-SiC, 197 meV at the hexagonal site in $4H$-SiC (Ref. 8)]. This picture, however, changes for the energetically more favorable tilted configuration. In this case two (three) LVM's at the cubic (hexagonal) site in good agreement with the values of the *P–T* centers are found (Sec. III A). Also the values of the frequency ratios for the high-frequency mode are in excellent agreement. This finding supports the split interstitial model of Evans *et al.*[6] Yet, some issues still have to be resolved: First, the ratios of the isotope shifts for the low-frequency LVM's (Table I) are smaller than that of the *P–T* centers, especially in $3C$-SiC. Second, the shifted frequencies and the ratios depend on the site of the substituted carbon atom. Third, two very close low-frequency modes are obtained at the hexagonal site. All these facts are not evident from the experimental data. However, the spectrum is very complex and difficult to resolve,[6] hence it is not unlikely that further weak peaks close to the reported vibrational modes may exist. A further difficulty is the high mobility of the carbon interstitial,[9] which is not compatible with the high annealing temperature of ≈ 1000 °C of the centers. Two explanations are possible: First, the carbon interstitials are trapped in interstitial clusters,[17] and re-emitted in the annealing process. If this is the case, it should be possible to anneal out the *P–T* centers at lower temperatures, but at longer annealing times. Second, the low-energy irradiation with a very high flux produces a large amount of carbon interstitials, which may not completely annihilate with vacancies during the annealing. The mobile interstitials migrate away from vacancies and maintain a metastable high concentration after the cooling. This interpretation is supported by the finding that the intensity especially of the *P* center drops very slowly outside the irradiated area.

The dicarbon antisite has been discussed as a possible model by Gali *et al.*[8] Mode 5 of $(C_2)_{Si}$ (cf. Table IV) has been associated with the high-frequency LVM of the *P–T* centers. Due to the localized character of this vibration of the carbon dumbbell, we observe a threefold isotope splitting, and the corresponding frequency ratios indeed agree very well with the experimental results. Modes 3 and 4 have been associated with the low-frequency LVM (the high-spin case has been considered in Ref. 8, where these two modes are degenerate). However, this assignment bears some difficulties. First, the energy difference between the symmetric high-spin case and the Jahn-Teller distorted low-spin case is too small to uniquely determine the true ground state configuration (80 meV in $3C$-SiC and 120 meV in $4H$-SiC in favor of the high-spin state).[5] Second, due to the lower crystal symmetry in $4H$-SiC the modes 3 and 4 are non-degenerate even in the high-spin case.[5] With its hexagonal-cubic-cubic stacking sequence the polytype $6H$-SiC has a similarly low

symmetry; thus it is likely that in $6H$-SiC modes 3 and 4 of the defect should also be observed independently. An experimental verification in PL measurements is possible by imposing a uniaxial pressure on a nonenriched crystal. The pressure favors the distorted configuration and thus the splitting of modes 3 and 4. Analyzing the isotope shifts of the modes 3 and 4, Gali *et al.* substituted the two dumbbell atoms with ^{13}C.[8] Hereby a twofold splitting of the degenerate mode (modes 3 and 4) was observed, in good agreement with experiment. However, the inclusion of the nearest-neighbor atoms in the isotope analysis has a significant impact on these modes. In the Jahn-Teller distorted configuration, the two lines split into two groups with six shifted lines in each (cf. Fig. 5). In the symmetric high-spin case the groups overlap and result in seven lines, which cannot be separated. Thus this model cannot explain the twofold splitting of the lower mode of the *P–T* centers. Mode 2 was declared invisible by Gali *et al.*[8] due to the defect's D_{2d} symmetry. However, in the Jahn-Teller distorted configuration the symmetry reduces to C_{2v} and in the hexagonal polytypes to C_{1h}. Similar arguments refer to isolated molecules,[34] which is not relevant in case of the dicarbon antisite. Yet, the dicarbon antisite could explain the thermal stability of the *P–T* centers of up to 1000 °C without referring to the cluster formation. The defect, however, needs carbon antisites as a prerequisite for its formation. Since the samples were irradiated with low-energy electrons, a decent concentration of antisites has to be created by kinetic processes, before the dicarbon antisite can form.

The five different ZPL's may originate from the various locations of the defect (either the dicarbon antisite or the split interstitial) at inequivalent sites in $6H$-SiC. Another explanation may be the excitation of the defect states in the band gap. The experiments have been performed with excitation energies below the SiC band gap;[6] hence it is likely that the bound excitons were formed by the excitation of an occupied defect state and not by trapping a free exciton. The energy of the ZPL may thus depend on the energetic position of the defect level in the band gap, which may vary with the location of the defect at a cubic or a hexagonal site. Also the generation of excited exciton states should be considered. This may be clarified with the measurement of relaxation times. The analysis performed in Ref. 6 of the centers' spatial distribution in the irradiated region and its boundary may also give an indication of the correlations between the various centers.

Both models (dicarbon antisite and carbon split interstitial) show properties that allow us to consider them as candidates for the *P–T* centers. However, both have difficulties that have to be resolved. Among the other defects that we studied, neither the interstitial clusters nor the antisite-related clusters can explain the *P–T* centers. Either the LVM pattern is incompatible with experiment or the isotope splitting. Considering all these results, the split interstitial appears to be the simplest and the most likely interpretation.

C. The *U* center

Besides the *P–T* centers Evans *et al.*[6] have found a center with a high-frequency mode at 246.6 meV which has been

labeled the U center. Further modes have not been identified in the spectra so far. In ^{13}C enriched material two shifted modes at 242.1 and 237.4 meV are observed, with the frequency ratios of 1.019 and 1.039, respectively. It has been speculated that the threefold splitting again originates from the carbon-carbon dumbbell vibrations. However, such a high vibrational frequency had not been observed for a carbon-based defect before. Also the frequency ratios do not perfectly fit the square root dependence on the mass ratios. LVM's with such high energies have been earlier identified as hydrogen or deuterium (C-H and C-D) vibrational modes at 369 and 274 meV, respectively.[35] Therefore Evans *et al.*[6] suggested that hydrogen may be involved in this defect center.

Yet, the calculations for the tricarbon antisite $(C_3)_{Si}$ and the tetracarbon antisite $(C_4)_{Si}$ (cf. Sec. IV C) show that LVM's up to 250 meV should be possible for purely carbon-based defects. For the tricarbon antisite, the highest mode at 248.5 meV is a strongly localized stretching vibration that shows a threefold isotope splitting with frequency ratios (1.018 and 1.036) close to that of the U center. Thus the relation of the U center to the carbon-carbon dumbbell is plausible. As discussed in Sec. IV C, the vibrations of the energetically lower modes of the tricarbon antisite are very complex and involve several carbon atoms, resulting in a strong isotope broadening of these lines. In the complex spectra presented in Ref. 6, additional low-frequency lines may be hidden. If the further lower modes of the U center were found, an identification of the U center with the tricarbon antisite would be a good possibility. The high dissociation energy of 4.8 eV in $3C$-SiC and 5.8 eV in $4H$-SiC can also explain the thermal stability of the U center, which has been observed up to 1300 °C.

Evans *et al.*[6] also discussed the spatial distribution of the U centers. Directly after irradiation the center has been observed, if at all, in the periphery of the irradiated region, and inside the region only after annealing above 1000 °C. The annealing behavior is completely different from that of the P-T centers. This finding supports our interpretation of the preceding section that the split-interstitials are responsible for the P-T centers, since the U center and the P-T centers must have a different origin. If we identified the P-T centers with the dicarbon antisite and the U center with the tricarbon antisite, the P-T centers should coexist in the same region, which apparently is not the case. The split-interstitial and the antisite defects are, however, fundamentally different defect configurations. The interpretation of the dicarbon antisite as a building block of the D_{II} center (cf. Sec. V A and Ref. 5) implies that also the tricarbon antisite should then be a precursor of the D_{II} center. If the tricarbon antisite is related to the U center, this should be observed in the experimental data. Indeed, the U center vanishes at 1300 °C, whereas the D_{II} center rises above these temperatures.[11] Careful annealing studies of the intrinsic PL centers could help to clarify the formation behavior of the various defects.

D. Comparison with carbon aggregation in diamond

In diamond, di-, tri- and tetra-interstitials have been considered by *ab initio* methods. Goss *et al.*[20] have found similar configurations to $(C_{sp})_2$, $(C_2)_{hex}$, $(C_{sp})_3$, and $(C_{sp})_4$. The defects possess a very rich vibrational spectrum above the diamond bulk phonon limit at 164 meV. The di-interstitials show six LVM's up to 228 meV [I_2 similar to $(C_{sp})_2$] and seven LVM's up to 243 meV [I_2 similar to $(C_2)_{hex}$]. The hexagonal di-interstitial thus shows a much higher frequency than I_2 based on two split interstitials, which is not so clearly visible in $3C$-SiC. The tri-interstitial I_3 shows 11 LVM's up to 216 meV and the tetra-interstitial I_4 12 LVM's up to 197 meV. It is observed that the frequencies are generally much higher than in SiC due to the shorter bond lengths of diamond. The overall behavior is very similar: the highest LVM goes down with an increase of the number of interstitial atoms, a feature that is also observed for the interstitial clusters in SiC (cf. Table III). The high number of LVM's has been obtained for the ring of dicarbon antisites $[(C_2)_{Si}]_4$, with all dumbbells enclosed by a pure carbon shell. For this defect 11 LVM's are counted instead of five for $(C_{sp})_4$, whereas the highest LVM does not differ considerably compared to $(C_{sp})_4$. Thus for the defects spanning several lattice sites only the number of LVM's appears to depend on the number of carbon atoms involved. The highest LVM frequency is determined by the crystal lattice.

Another similarity of SiC and diamond is the increase of the dissociation energy per atom with the cluster size. The cluster dissociation energy is defined in Ref. 20 as $E_D = nE_f(I_1) - E_f(I_n)$, where n is the cluster size. For the di-interstitials, this definition gives the same values as listed in Table II. For the tri- and tetra-interstitial we obtain 5.8 and 11.5 eV, respectively. The increase of the dissociation energy can be attributed to the larger number of sp^3-hybridized carbon atoms in the defect.

The comparison with diamond shows that defects with a high vibrational frequency (tricarbon and tetracarbon antisite) may exist in SiC. Since they are confined at a single lattice site, they are only weakly influenced by the surrounding lattice. The short carbon-carbon bonds give rise to high-frequency LVM's as in diamond.

VI. SUMMARY AND CONCLUSION

We investigated the energetic, structural, and vibrational properties of small carbon clusters in $3C$- and $4H$-SiC. We considered two different types of aggregates. One type is clusters of carbon interstitials, where we investigated clusters with up to four interstitials. The other type is a collection of carbon atoms at carbon-antisite positions. Clusters comprised of up to four carbon atoms at a silicon site were found. Due to their short carbon-carbon bonds and their light carbon constituents they reveal vibrational modes well above the SiC bulk phonon spectrum. We analyzed the vibrational signatures as well as the isotope shifts of the defects by *ab initio* calculations and compared them with the photoluminescence centers P-T, U, and D_{II}. As the origin of the P-T centers, the carbon split interstitial and the dicarbon antisite were discussed. Both defects possess LVM's at appropriate frequencies. The isotope shifts of the high-frequency mode of the P-T centers are in good agreement with the results for both defects. Yet, the twofold isotope splitting of the low-

frequency mode cannot be explained by the dicarbon antisite, which shows an at least sixfold splitting for the modes in that frequency range. For the split interstitial the isotope splitting of the low-frequency mode is compatible with experiment. None of the other interstitial and antisite clusters showed such a clear isotope splitting as observed for the P-T centers.

The highly mobile carbon interstitials can aggregate and form stable carbon interstitial clusters. The signatures of di-, tri- and tetra-interstitials were presented. The most stable form of the di-interstitial is the hexagonal di-interstitial $(C_2)_{hex}$. This defect possesses an LVM spectrum which is practically independent of the polytype and in $4H$-SiC also insensitive to variations of the configuration. The highest LVM of interstitial clusters reduces with the number of split interstitials involved—a behavior that is consistent with similar defects in diamond. Only very compact interstitial clusters as $[(C_2)_{hex}]_2$ can have high-frequency LVM's. Carbon aggregates may also affect the annealing processes of intrinsic defects. They can trap mobile carbon interstitials and re-emit them again at higher temperatures and thus provide the constituents for further stable defect centers. The apparent contradiction in the identification of the thermally stable P-T centers with a highly mobile split interstitial may be lifted in this way.

Also the carbon antisite may trap carbon interstitials. This may result in very compact defect clusters with LVM's up to 255 meV, which was obtained for $(C_3)_{Si}$ in $4H$-SiC. Consequently, defect centers like the U center may be entirely carbon based. Also, complexes of neighboring antisites may form. Examples are the pair of dicarbon antisites $[(C_2)_{Si}]_2$ and the ring of dicarbon antisites $[(C_2)_{Si}]_4$. These defects behave similar to the split interstitial clusters, yet they show a richer spectrum. The relevance of these complexes for the D_{II} center was discussed. The compact antisite clusters cause LVM's well above 200 meV, whereas the complexes spanning several defect sites have energetically lower, but richer spectra. Thus for the D_{II} center an extended defect that grows on the dicarbon antisite as core structure may be the origin. This implies that simple defects like the dicarbon antisite should be observed experimentally as a precursor of the D_{II} center.

The centers P-U and D_{II} are yet the only experimentally observed intrinsic defects with LVM's above the SiC bulk phonon spectrum. We have presented various stable defect configurations with high-frequency LVM's. This indicates that probably a number of new defect centers shall be discovered in future experiments.

*Electronic address: Alexander.Mattausch@physik.uni-erlangen.de

[1] L. Patrick and W. J. Choyke, Phys. Rev. B **5**, 3253 (1972).

[2] L. Patrick and W. J. Choyke, J. Phys. Chem. Solids **34**, 565 (1973).

[3] A. Gali, P. Deák, E. Rauls, N. T. Son, I. G. Ivanov, F. H. C. Carlsson, E. Janzén, and W. J. Choyke, Phys. Rev. B **67**, 155203 (2003).

[4] T. A. G. Eberlein, C. J. Fall, R. Jones, P. R. Briddon, and S. Öberg, Phys. Rev. B **65**, 184108 (2002).

[5] A. Mattausch, M. Bockstedte, and O. Pankratov, Phys. Rev. B **69**, 045322 (2004).

[6] G. A. Evans, J. W. Steeds, L. Ley, M. Hundhausen, N. Schulze, and G. Pensl, Phys. Rev. B **66**, 035204 (2002).

[7] J. W. Steeds (private communication).

[8] A. Gali, P. Deák, P. Ordejón, N. T. Son, E. Janzén, and W. J. Choyke, Phys. Rev. B **68**, 125201 (2003).

[9] M. Bockstedte, A. Mattausch, and O. Pankratov, Phys. Rev. B **68**, 205201 (2003).

[10] A. Mattausch, M. Bockstedte, and O. Pankratov, Mater. Sci. Forum **353–356**, 323 (2001).

[11] J. A. Freitas, S. G. Bishop, J. A. Edmond, J. Ryu, and R. F. Davis, Appl. Phys. Lett. **61**, 2011 (1987).

[12] T. T. Petrenko, T. L. Petrenko, and V. Y. Bratus, J. Phys.: Condens. Matter **14**, 12433 (2002).

[13] M. Bockstedte, M. Heid, and O. Pankratov, Phys. Rev. B **67**, 193102 (2003).

[14] M. Bockstedte, M. Heid, A. Mattausch, and O. Pankratov, Mater. Sci. Forum **433–436**, 471 (2003).

[15] H. Itoh, A. Kawasuso, T. Ohshima, M. Yoshikawa, I. Nashiyama, S. Tanigawa, S. Misawa, H. Okumura, and S. Yoshida, Phys. Status Solidi A **162**, 173 (1997).

[16] N. Son, P. Hai, and E. Janzén, Mater. Sci. Forum **353–356**, 499 (2001).

[17] M. Bockstedte, A. Mattausch, and O. Pankratov, Phys. Rev. B **69**, 235202 (2004).

[18] D. J. Eaglesham, P. A. Stolk, H.-J. Gossmann, and J. M. Poate, Appl. Phys. Lett. **65**, 2305 (1994).

[19] A. M. Stoneham, *Theory of Defects in Solids* (Oxford University Press, London, 1975).

[20] J. P. Goss, B. J. Coomer, R. Jones, T. D. Shaw, P. R. Briddon, M. Rayson, and S. Öberg, Phys. Rev. B **63**, 195208 (2001).

[21] M. Bockstedte, A. Kley, J. Neugebauer, and M. Scheffler, Comput. Phys. Commun. **107**, 187 (1997).

[22] P. Hohenberg and W. Kohn, Phys. Rev. **136**, 864 (1964).

[23] W. Kohn and L. J. Sham, Phys. Rev. **140**, 1133 (1965).

[24] J. P. Perdew and A. Zunger, Phys. Rev. B **23**, 5048 (1981).

[25] H. J. Monkhorst and J. D. Pack, Phys. Rev. B **13**, 5188 (1976).

[26] A. Mattausch, M. Bockstedte, and O. Pankratov, Physica B **308–310**, 656 (2001).

[27] A. Gali, P. Deák, N. T. Son, and E. Janzén, Mater. Sci. Forum **389–393**, 477 (2002).

[28] A. Mattausch, M. Bockstedte, and O. Pankratov, Mater. Sci. Forum **389–393**, 481 (2002).

[29] E. Rauls, T. Frauenheim, A. Gali, and P. Deák, Phys. Rev. B **68**, 155208 (2003).

[30] T. Egilsson, A. Henry, I. G. Ivanov, J. L. Lindström, and E. Jan-

zén, Phys. Rev. B **59**, 8008 (1999).

[31] S. G. Sridhara, D. G. Nizhner, R. P. Devaty, W. J. Choyke, T. Dalibor, G. Pensl, and T. Kimoto, Mater. Sci. Forum **264–268**, 493 (1998).

[32] F. H. C. Carlsson, S. G. Sridhara, A. Hallén, J. P. Bergman, and E. Janzén, Mater. Sci. Forum **433–436**, 345 (2003).

[33] S. G. Sridhara, F. H. C. Carlsson, J. P. Bergman, A. Henry, and E. Janzén, Mater. Sci. Forum **353–356**, 377 (2001).

[34] R. B. Capaz, A. Dal Pino, and J. D. Joannopoulos, Phys. Rev. B **58**, 9845 (1998).

[35] W. J. Choyke and L. Patrick, Phys. Rev. Lett. **29**, 355 (1972).